Influence of Density on Properties of Compressed Weeping Willow (*Salix babylonica*) Wood Panels

Neng Li Minzhen Bao Yuhe Chen Yamei Zhang
Yongjie Bao Wenji Yu

Abstract

Compressed wood panels (CWP) is a biomaterial that can potentially address common issues with fast-growing wood, including low density, high perishability, and low mechanical strength. As wood density is known to significantly affect material properties, this study examines the cellular structure, wettability, physicomechanical performance, water absorption (WA), and dimensional stability of compressed weeping willow wood panels (CWWWP) at various densities. The cellular structure was investigated by a scanning electron microscope, and major physicomechanical properties were also measured, i.e., modulus of rupture, modulus of elasticity, and horizontal shear strength. Contact angle measurements and surface free-energy (SFE) calculations were used to elucidate CWWWP wettability. The experimental results showed that the cellular deformation, composite strength, and volume-swelling efficiency all tended to increase with increasing density. However, both the SFE and WA were negatively correlated with the CWWWP density. This study concludes that higher-density CWWWP, with better mechanical performance and lower WA, is suitable for structural wood products and engineering materials, whereas lower-density CWWWP is suited for use as decorative material because of its lower density and higher SFE, which increases the ease of coating and painting.

Wood is recognized as a sustainable biomaterial and is widely used because of its attractive natural color, beautiful texture, ease of processing, and high strength-to-weight ratio (Li et al. 2015). The increasing demand for wood products and the decreasing supply has prompted the development of planted forests and fast-growing forests. China has the largest area of planted forest in the world (Chinese Forestry Administration 2012). However, most fast-growing wood comes with a set of characteristics, including low density, high perishability, and low mechanical strength, that present challenges for utilization. Therefore, it is essential to develop nontraditional materials from them with improved physical and mechanical properties and improved water absorption (WA) to create additional value.

Compressed wood panels (CWP) is a good choice for nontraditional material; it is a wood-based composite similar to the ‘‘compreg’’ process formed via veneers impregnated with a water-soluble phenol-formaldehyde (PF) resin, and then reformed into the desired shape (Yalinkilic et al. 1999, Bekhta et al. 2009, Unsal et al. 2009, Sulaiman et al. 2012). CWP could meet the requirements of different mechanical strength by changing the degree of compression. The investigation of Roh and Ra (2009) demonstrated that the mechanical properties tended to increase with an increase in density of the veneer–bamboo zephyr composite. A similar result was observed in the research of a bamboo fibrous sheet composite (Zhu and Yu 2011). Moreover, a negative correlation was found to exist between the composite density and the thickness swelling (Yu et al. 2015).

The objective of this study was to determine the effect of density on compressed weeping willow wood panel

The authors are, respectively, Assistant Professor, Research Inst. of Wood Industry, Chinese Acad. of Forestry, Beijing; Dept. of Wood Sci. and Technol., Beijing Forestry Univ., Beijing, China; China National Bamboo Research Center, and Key Lab. of High Efficient Processing of Bamboo of Zhejiang Province, Hangzhou (lineng8657@sina.com); Doctoral Candidate, Research Inst. of Wood Industry, Chinese Acad. of Forestry, Beijing (bomithen@126.com); Professor, China National Bamboo Research Center, and Key Lab. of High Efficient Processing of Bamboo of Zhejiang Province, Hangzhou (yuhec@sina.com); Assistant Professor, Research Inst. of Wood Industry, Chinese Acad. of Forestry, Beijing (zhangyamei20060918@126.com); Assistant Professor, Research Inst. of Wood Industry, Chinese Acad. of Forestry, Beijing; China National Bamboo Research Center, and Key Lab. of High Efficient Processing of Bamboo of Zhejiang Province, Hangzhou (baoyongjie1@126.com); and Professor, Research Inst. of Wood Industry, Chinese Acad. of Forestry, Beijing; and China National Bamboo Research Center, Hangzhou (yuwenji@caf.ac.cn [corresponding author]). This paper was received for publication in April 2016. Article no. 16-00018.

Forest Prod. J. 67(1/2):44–49.
doi:10.13073/FPJ-D-16-00018

(CWWWP) properties, including microscopic structure, wettability, mechanical properties, WA, and dimensional stability. Weeping willow veneer (WWV), arranged by grain in a parallel direction and with varying thicknesses, was used to form CWWWP at various panel densities. Microscopic structure observation was investigated by scanning electron microscopy (SEM). The mechanical and physical properties were evaluated through the modulus of rupture (MOR), modulus of elasticity (MOE), horizontal shear (HS) strength, WA, and volume-swelling efficiency (VSE). The detection of wettability was by contact angle (CA) measurement and surface free-energy (SFE) calculations.

Materials and Methods

The WWV, with an air density of 0.39 g/cm^3, a moisture content of 3.5 percent, and a thickness in the range of 0.6 to 2.4 mm, obtained by rotary cutting (Kexingyu Machinery Manufacturing Co., Ltd., China), was studied. Before the application of PF resin, WWVs were cut into rectangular (280 by 10-mm) veneers. The rectangular WWVs were then soaked in a 20 percent PF solution for several minutes to achieve 10 percent resin content. The original, prediluted PF possessed a solid content of 46.2 percent, a viscosity of 36 mPa·s at 23°C, and a pH of 10 to 11 (Beijing Taier Chemical Co., Ltd., China). Equation 1 was used to calculate the resin content:

$$C = \frac{(m_2 - m_1) \times w}{m_1 \times (1 - x)} \tag{1}$$

where C is the resin content; m_1 and m_2 are, respectively, the WWV weight pre- and postimmersion in the resin; w is the solid resin content; and x is the wet-basis moisture content preresin immersion.

The WWVs treated by PF immersion were oven-dried at 55°C until they reached a moisture content of approximately 10 percent. The designed densities of 0.5 to 1.1 g/cm^3 were achieved by controlling the weight of the resin-impregnated WWVs after drying. The WWVs were then transferred to a single-opening hydraulic hot press (Carver, USA), with all veneers arranged in a parallel-to-grain direction, and pressed at a hot platen temperature of 140°C for 6 minutes, resulting in CWWWP with target densities of 0.50 to 1.10 g/cm^3. Five replicates were established for each density of CWWWP. The composites were edge-cut in panels of 260 by 8 mm, and smaller samples were cut depending on what was needed to measure specific physicomechanical properties. The composite sample densities for measuring physical and mechanical properties and water absorption and dimensional stability with six replicates are presented in Table 1.

Microscopic observation was performed using SEM (S-4700, Hitachi, Japan) with an accelerating voltage of 15 kV. After being treated with purified water (Sample a, immersion for 6 h; Sample c, immersion for 18 h; Sample e, immersion for 30 h; Sample g, immersion for 42 h), cross sections of CWWWP were obtained by a slicer (HM 430, Microm, Germany) to expand the samples for better observation. Before SEM investigation, the cross sections were gold-palladium coated in a vacuum sputter coater.

The specimens were cut into slides with dimensions of 25 by 25 by 6 mm. Before measuring the CA, the board surface was sanded. Grit paper of 100, and finally 180, was used in sequence. Sample CAs were determined by the sessile drop method with a CA analyzer (DSA 100, Kruss, Germany). Water, formamide, and diiodomethane were the test liquids. Data collection began as soon as the test droplets were detected to have touched the wood surface; this typically occurred within zero to three frames (one frame $\approx$ 19.2 ms). All CA data were collected within 60 seconds from the starting point of measurement.

The SFE components of the testing liquids according to Fombuena et al. (2013) and Wang et al. (2015) are presented in Table 2. The SFE of samples with various densities was calculated according to the Lifshitz–van der Waals acid-base approach (Van Oss et al. 1988). As Bryne and Wålinder (2010) suggested, the SFE of samples can be calculated from the initial CAs of water (polar), formamide (polar), and diiodomethane (nonpolar) according to Equations 2, 3, and 4:

$$\gamma_S = \gamma_S^{LW} + \gamma_S^{AB} \tag{2}$$

$$\gamma_S^{AB} = 2\sqrt{\gamma_S^+ \gamma_S^-} \tag{3}$$

$$(1 + \cos\theta)\gamma_L = 2\left(\sqrt{\gamma_S^{LW}\gamma_L^{LW}} + \sqrt{\gamma_S^+ \gamma_L^-} + \sqrt{\gamma_S^- \gamma_L^+}\right) \tag{4}$$

where γ_S is the CWWWP SFE (mJ m^{-2}), γ_S^{LW} is the apolar (Lifshitz–van der Waals) component of CWWWP SFE (mJ m^{-2}), γ_S^{AB} is is the polar (Lewis acid-base) component of CWWWP SFE (mJ m^{-2}), γ_S^+ is the electron-accepting component of CWWWP acid–base components (mJ m^{-2}), γ_S^- is the electron-donating component of CWWWP acid-base components (mJ m^{-2}), θ is the liquid CA on CWWWP (°), γ_L^{LW} is the apolar component of liquid SFE (mJ m^{-2}), γ_S^+ is the electron-accepting component of liquid acid-base components (mJ m^{-2}), and γ_S^- is the electron-donating component of liquid acid-base components (mJ m^{-2}).

The panels were cut into smaller specimens, 120 by 15 by 6 mm for MOR and MOE and 60 by 15 by 6 mm for HS. According to the National Standard of China GB/T 17657

Table 1.—Observed densities of compressed weeping willow wood panel samples.

Properties[a]	Values (g/cm^3) for each sample						
	a	b	c	d	e	f	g
SEM	0.50	—	0.71	—	0.89	—	1.08
CA/SFE	0.50	0.61	0.70	0.79	0.90	1.01	1.10
MOR/MOE	0.50 ± 0.009	0.60 ± 0.014	0.70 ± 0.011	0.81 ± 0.014	0.90 ± 0.014	1.01 ± 0.008	1.08 ± 0.017
HS strength	0.50 ± 0.009	0.60 ± 0.010	0.70 ± 0.007	0.80 ± 0.009	0.90 ± 0.012	1.00 ± 0.014	1.11 ± 0.007
WA/VSE	0.50 ± 0.007	0.60 ± 0.011	0.70 ± 0.013	0.78 ± 0.009	0.90 ± 0.009	1.00 ± 0.012	1.08 ± 0.016

[a] SEM = scanning electron microscopy; CA/SFE = contact angle/surface free energy; MOR/MOE = modulus of rupture/modulus of elasticity; HS = horizontal shear; WA/VSE = water absorption/volume swelling efficiency.

Table 2.—Values of Lifshitz–van der Waals (γ_L^{LW}), electron acceptor (γ_L^+), and electron donor (γ_L^-) components of the test liquids.

Test liquid	Surface free energy (mJ m^{-2})			
	γ_L	γ_L^{LW}	γ_L^+	γ_L^-
Water	72.8	21.8	25.5	25.5
Formamide	58.0	39.0	2.28	39.6
Diiodomethane	50.8	50.8	0	0

(Chinese National Standardization Management Committee [CSMC] 2013), static bending tests were conducted on seven specimens, using a three-point bending test over 15 times at a 90-mm span at a loading speed of 5 mm/min. The MOR and MOE were measured parallel to the face grain. The HS was performed using the National Standard of China GB/T 20241 (CSMC 2006).

The moisture samples were first conditioned in a room with a controlled atmosphere at a temperature of 20°C ± 2°C and a relative humidity of 65 ± 5 percent until they reached a constant mass, and then the weights and dimensions of the samples were tested. The samples with six replicates in each group were placed in a water bath kettle filled with deionized water at a temperature of 63°C. The weights and dimensions of the samples were tested after 12, 24, 48, and 96 hours of immersion, and the WA and VSE were calculated as the index of dimensional stability according to Equations 5 and 6:

$$\mathrm{WA}_n\ (\%) = \frac{W_n - W_i}{W_i} \times 100 \tag{5}$$

$$\mathrm{VSE}_n\ (\%) = \frac{V_n - V_i}{V_i} \times 100 \tag{6}$$

where W_n is the weight of the sample after n hours of immersion, W_i is the weight of the original sample, V_n is the volume of the sample after n hours of immersion, and V_i is the volume of the original sample.

Results and Discussion

Figure 1 shows the SEM micrographs of the cross sections of the samples. The pore, fiber tracheid, wood ray, and axial parenchyma are easily observed in Figure 1a, and all of that tissue retained its original shape. A slight deformation of the wood cell was visible in the SEM micrographs of the samples with 0.71 g/cm^3 densities. Those images were taken after the first compression with hot pressing and then the expansion with water immersion. More cell shape distortion was observed with 0.89 g/cm^3 densities, as can be seen in Figure 1e, and the worst deformation is shown in Figure 1g. It can be deduced that the degree of CWWWP deformation tended to increase with an increase in the sample density. This phenomenon is likely because of the pressure applied to achieve different densities, in combination with the large cell lumen and thin cell walls of major cellular elements, e.g., vessels, vascular tracheids, wood rays, and axial parenchyma. These high pressures and temperatures of the hot press easily reshaped the tissue by decreasing the space of the cell lumen, resulting in more cell wall material per unit volume and thus, an increased density.

The wettability of CWWWP with various densities was measured by CA and SFE tests. Figure 2 shows a plot evolution of the CA variation in terms of different densities.

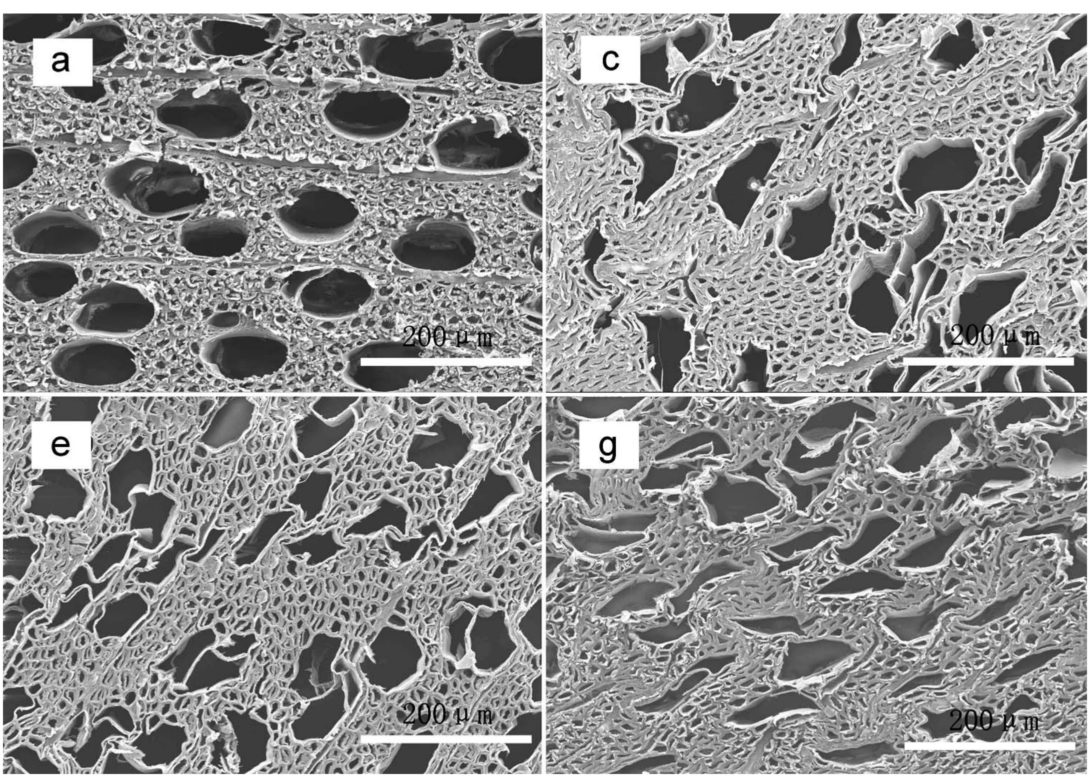

Figure 1.—Scanning electron microscopy images of compressed weeping willow wood panels (Sample a, density 0.50 g/cm^3; Sample c, density 0.71 g/cm^3; Sample e, density 0.89 g/cm^3; Sample g, density 1.08 g/cm^3).

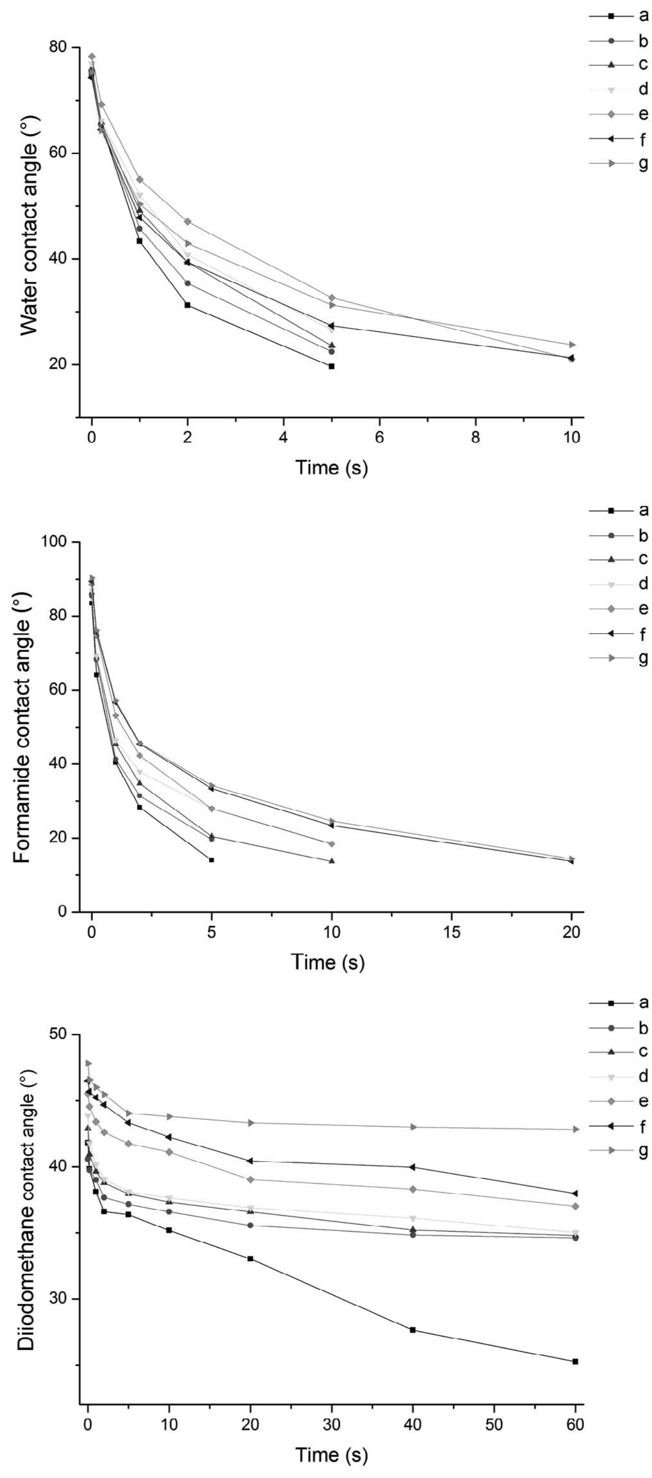

Figure 2.—Time-dependent contact angles of compressed weeping willow wood panels with various liquids and densities (samples: a, 0.50 g/cm^3; b, 0.61 g/cm^3; c, 0.70 g/cm^3; d, 0.79 g/cm^3; e, 0.90 g/cm^3; f, 1.01 g/cm^3; g, 1.10 g/cm^3).

Table 3 lists the initial CAs of CWWWP, which measured the moment that the machine detected the CA, which was after the testing droplets touched the surface. All the CAs with seven different densities exhibited slight differences in the initial CAs, which were approximately 74.26° to 78.33°. However, the differences in the CAs among the samples increased with extension of time that the water droplet remained on the sample surface. The maximum initial CA, measured by water, was obtained for CWWWP Sample e (density, 0.90 g/cm^3). Nevertheless, the descent rate of Sample e was larger than that of Sample g, which displayed the maximum CA after 10 seconds.

Table 3.—Initial contact angles of compressed weeping willow wood panels with various liquids and densities.[a]

Samples	Contact angles (°) for each liquid: Water	Formamide	Diiodomethane
a	74.86	83.49	41.81
b	75.52	85.45	40.58
c	75.98	86.32	42.89
d	76.93	86.93	43.89
e	78.33	88.62	45.54
f	74.26	89.47	46.50
g	75.27	90.36	47.83

[a] Panel densities: a, 0.50 g/cm^3; b, 0.61 g/cm^3; c, 0.70 g/cm^3; d, 0.79 g/cm^3; e, 0.90 g/cm^3; f, 1.01 g/cm^3; and g, 1.10 g/cm^3.

Both the formamide and diiodomethane tests revealed that the initial CAs tended to decrease with increasing density. The maximum initial CAs by formamide and diiodomethane were obtained for Sample g, with a density of 1.10 g/cm^3, which gives a better lyophobicity protection for CWWWP, and the CA values were 90.36° and 47.83°, respectively. Similar to the results with water, differences in the CAs measured by formamide and diiodomethane increased with the increasing amount of time on the sample surface, with most of the curves falling sharply. However, the curve for Sample g (1.10 g/cm^3), measured by diiodomethane, remained stable after 5 seconds. In general, higher-density samples showed fewer changes in CA over time. This outcome is probably because of the decreased cell lumen size in these samples, according to the results of SEM. Alternatively, the cell could reshape and the cell lumen space could be reduced in the higher-density samples, resulting in a decrease in absorption and absorption rate.

The SFE is a reflection of the surface molecular interatomic forces and is closely related to the solid surface wettability. It is well known that some industrial applications, such as coating, painting, and the formation of adhesion joints, require high SFE to promote good bonding (Fombuena et al. 2013). It is important to investigate the change of CWWWP surface energy with different densities. The SFE components of CWWWP calculated on the basis of the initial CA data are presented in Table 4. It can be

Table 4.—Surface energies and the Lifshitz–van der Waals (γ_S^{LW}), electron acceptor (γ_S^+), and electron donor (γ_S^-) components of compressed weeping willow wood panels with different densities.[a]

Samples	Surface free energy (mJ m^{-2}): γ_S	γ_S^{LW}	γ_S^+	γ_S^-
a	18.785	18.780	0.000	11.949
b	17.844	17.827	0.000	10.421
c	17.459	17.455	0.000	9.956
d	17.145	17.141	0.000	9.629
e	17.298	16.828	−0.006	9.358
f	16.658	16.027	−0.011	8.941
g	15.255	15.250	0.000	8.544

[a] Panel densities: a, 0.50 g/cm^3; b, 0.61 g/cm^3; c, 0.70 g/cm^3; d, 0.79 g/cm^3; e, 0.90 g/cm^3; f, 1.01 g/cm^3; and g, 1.10 g/cm^3.

clearly observed that the SFE decreases as the density increases; the same variation tendencies are observed for γ_L^{LW} and γ_L^{-} Sample a, with a density of 0.50 g/cm^3, had the highest SFE, 18.785 mJ/m^2, followed by Sample b, with a density of 0.61 g/cm^3. Sample g, with a density of 1.10 g/cm^3, had the lowest SFE, 15.255 mJ/m^2. These results indicate that density increases in CWWWP are disadvantageous for material coating and painting applications.

The average values of the MOE and MOR, with standard deviations of CWWWP with seven different densities, are summarized in Figure 3. The bending properties increased with increasing CWWWP density. In addition, the rate increase of the MOR was greater than that of the MOE. The value of the MOR and MOE with different densities increased from 73.2 MPa (0.50 g/cm^3) to 189.5 MPa (1.08 g/cm^3), and from 7,354.4 MPa (0.50 g/cm^3) to 11,586.6 MPa (1.08 g/cm^3) as the density increased, respectively. These results can be rationalized by the fact that higher-density composites had more polymer per unit volume, thus exhibiting better contact between plies after hot pressing, compared with lower-density boards (Roh and Ra 2009, Zhu and Yu 2011). Notably, all failures of the test specimens in the bending tests occurred at the veneer, except in the lower-density Samples a and b. Within these samples, 66.7 percent of Sample a bond failures and 16.7 percent of Sample b

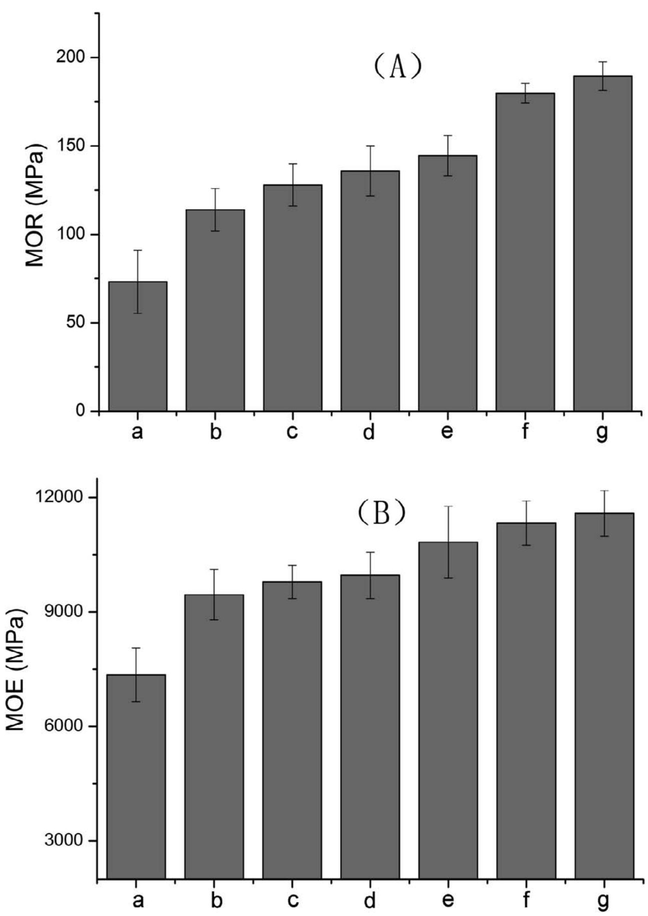

Figure 3.—Bending properties of compressed weeping willow wood panels with various densities (samples: a, 0.50 g/cm^3; b, 0.60 g/cm^3; c, 0.70 g/cm^3; d, 0.81 g/cm^3; e, 0.90 g/cm^3; f, 1.01 g/cm^3; g, 1.08 g/cm^3). (A) Modulus of rupture (MOR); (B) modulus of elasticity (MOE).

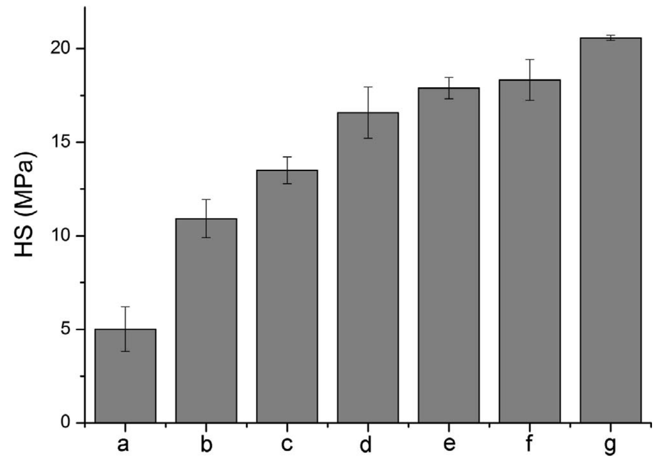

Figure 4.—Horizontal shear (HS) strength of compressed weeping willow wood panels with various densities (samples: a, 0.50 g/cm^3; b, 0.60 g/cm^3; c, 0.70 g/cm^3; d, 0.80 g/cm^3; e, 0.90 g/cm^3; f, 1.00 g/cm^3; g, 1.11 g/cm^3).

bond failures were observed at the glue lines. This outcome supports previous data showing that higher-density composites possess better internal strength (Roh and Ra 2009).

Figure 4 shows the HS strength of CWWWP with various densities. The trends were similar for the HS and bending strength tests. As the density increased from 0.50 to 1.11 g/cm^3, the HS increased from 5.0 to 20.6 MPa. The results of the HS further confirm the fact that high density has a positive effect on the mechanical properties related to material strength, primarily because of the resin impregnation along with increased fiber aggregation per unit volume at higher densities.

The WA of samples with various densities is presented in Figure 5. The change in the WA data after 96 hours of immersion at a temperature of 63°C for all samples shows a rising tendency. Across all samples, Sample a exhibited the largest rise in WA over time. The WA data of Sample a increased from 106.5 percent after 12 hours of immersion to 134.3 percent after 96 hours of immersion. In the first 12 hours of immersion, the WA changes are more pronounced.

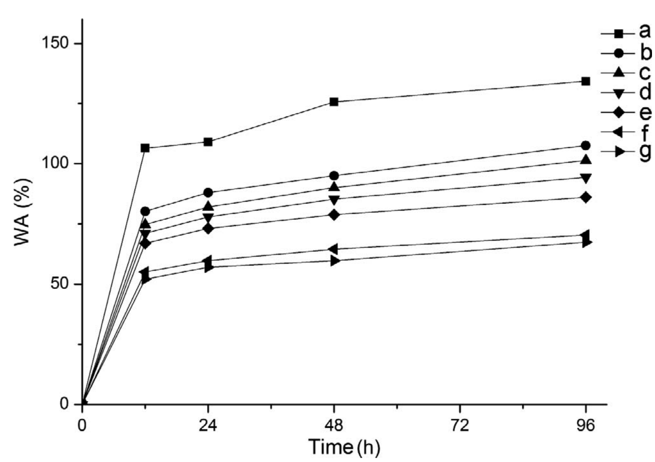

Figure 5.—Water absorption (WA) of compressed weeping willow wood panels with various densities (samples: a, 0.50 g/cm^3; b, 0.60 g/cm^3; c, 0.70 g/cm^3; d, 0.78 g/cm^3; e, 0.90 g/cm^3; f, 1.00 g/cm^3; g, 1.08 g/cm^3).

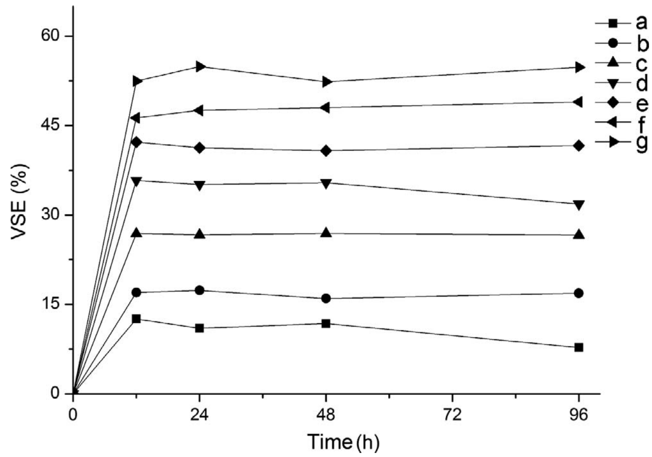

Figure 6.—Volume-swelling efficiency (VSE) of compressed weeping willow wood panels with various densities (samples: a, 0.50 g/cm^3; b, 0.60 g/cm^3; c, 0.70 g/cm^3; d, 0.78g/cm^3; e, 0.90 g/cm^3; f, 1.00 g/cm^3; g, 1.08 g/cm^3).

Sample g showed the smallest growth, followed by Samples f and e. The WA data of Sample g increased from 52.1 percent after 12 hours of immersion to 67.4 percent after 96 hours of immersion. The WA value of Sample g was approximately half of the WA value of Sample a. From Figure 5, it can be seen that a negative correlation between the density and the data of WA exists. Zhu and Yu (2011) made similar observations. Interestingly, the net water absorption ($W_n - W_i$) increased with an increase in density. More than likely, the denominator's (W_i) rapid growth obscured the influence of the numerator's ($W_n - W_i$) increase on WA.

The changes in the VSE of the samples are illustrated in Figure 6. In the first 12 hours of immersion, important changes in the VSE for all samples were observed, and remained stable thereafter. Finally, the smallest values of VSE were obtained for Samples a (7.8%), b (16.9%), and c (26.6%), which give a better dimensional stabilization than Sample d, where the VSE value was 31.8 percent. Sample g had the largest VSE of 54.8 percent, followed by Sample f with 49.0 percent and Sample e with 41.7 percent, indicating that their dimensional stability was the weakest. In summary, a noticeable tendency was observed in that the VSE value increased with an increase in density. This result indicated that increases in CWWWP density are not conducive to the dimensional stability. Positive correlation between the density and the VSE value is possibly caused by the greater spring-back of the compacted WWV in the high-density composite.

Conclusions

In this study, we investigated microscopic structure, wettability, physical and mechanical performances, WA, and dimensional stability of CWWWP. It has been shown that density had a significant effect on these properties. Specifically, the degree of CWWWP deformation, the value of MOR, MOE, HS, and VSE tended to increase with increasing density. A similar tendency was found in initial CAs with testing liquids of formamide and diiodomethane. Negative correlation was noticed in SFE and WA with density of CWWWP. High pressures and temperatures of the hot press easily reshaped the tissue by decreasing the space of the cell lumen, resulting in more cell wall material per unit volume. The increasing fiber aggregation per unit volume at higher densities increased the mechanical strength. The reduction of cell lumen space in the higher-density samples resulted in a decrease in absorption and absorption rate. The higher-density CWWWP exhibits greater mechanical performances and lower WA, making it suitable for structural wood products and engineering material. In contrast, lower-density CWWWP is more suited for decorative material because of its lower density and higher SFE, which makes it easier to coat, bond, and paint.

Acknowledgments

This work was supported by the Special Public Welfare Forestry Industry Research Project under grants 201404503 and 201404505 and the Science and Technology Planned Projects of Zhejiang Province under grants 2016F50006 and 2015F50054.

Literature Cited

Bekhta, P., S. Hiziroglu, and O. Shepelyuk. 2009. Properties of plywood manufactured from compressed veneer as building material. *Mater. Design* 30:947–953.

Bryne, L. E. and M. E. P. Wålinder. 2010. Ageing of modified wood. Part 1: Wetting properties of acetylated, furfurylated, and thermally modified wood. *Holzforschung* 64(3):295–304.

Chinese Forestry Administration. 2012. Chinese Forestry Statistical Yearbook. Chinese Forestry Publishing House, Beijing.

Chinese National Standardization Management Committee (CSMC). 2006. Laminated veneer lumber. GB/T 20241-2006. CSMC, Beijing.

Chinese National Standardization Management Committee (CSMC). 2013. Test methods of evaluating the properties of wood-based panels and surface decorated wood-based panels. GB/T 17657-2013. CSMC, Beijing.

Fombuena, V., J. Balart, T. Boronat, L. Sánchez-Nácher, and D. Garcia-Sanoguera. 2013. Improving mechanical performance of thermoplastic adhesion joints by atmospheric plasma. *Mater. Design* 47:49–56.

Li, N., Y. Chen, Y. Bao, Z. Zhang, Z. Wu, and Z. Chen. 2015. Evaluation of UV-permeability and photo-oxidisability of organic ultraviolet radiation-absorbing coatings. *Appl. Surf. Sci.* 332:186–191.

Roh, J. K. and J. B. Ra. 2009. Effect of moisture content and density on the mechanical properties of veneer–bamboo zephyr composites. *Forest Prod. J.* 59(3):75–78.

Sulaiman, O., N. Salim, N. A. Nordin, R. Hashim, M. Ibrahim, and M. Sato. 2012. The potential of oil palm trunk biomass as an alternative source for compressed wood. *BioResources* 7:2688–2706.

Unsal, O., S. N. Kartal, Z. Candan, R. A. Arango, C. A. Clausen, and F. Green III. 2009. Decay and termite resistance, water absorption and swelling of thermally compressed wood panels. *Int. Biodeterior. Biodegrad.* 63:548–552.

Van Oss, C. J., M. K. Chaudhury, and R. J. Good. 1988. Interfacial Lifshitz–van der Waals and polar interactions in macroscopic systems. *Chem. Rev.* 88(6):927–941.

Wang, W., Y. Zhu, J. Cao, and X. Guo. 2015. Thermal modification of Southern pine combined with wax emulsion preimpregnation: Effect on hydrophobicity and dimensional stability. *Holzforschung* 69(4):405–413.

Yalinkilic, M. K., I. Yuji, T. Munezoh, D. Zafer, and C. Y. Ahmet. 1999. Biological, mechanical, and thermal properties of compressed-wood polymer composite (CWPC) pretreated with boric acid. *Wood Fiber Sci.* 31:151–163.

Yu, H. X., C. R. Fang, M. P. Xu, F. Y. Guo, and W. J. Yu. 2015. Effects of density and resin content on the physical and mechanical properties of scrimber manufactured from mulberry branches. *J. Wood Sci.* 61(2):159–164.

Zhu, R. X. and W. J. Yu. 2011. Effect of density on physical and mechanical properties of reconstituted small-sized bamboo fibrous sheet composite. *Adv. Mater. Res.* 150:634–639.